Evidence for Antisymmetric Exchange in Cuboidal [3Fe−4S]$^{+}$ Clusters

Yiannis Sanakis,[†,‡] Anjos L. Macedo,[§] Isabel Moura,[§] Jose J. G. Moura,[§] Vasilios Papaefthymiou,[||] and Eckard Münck*,[†]

Contribution from the Department of Chemistry, Carnegie Mellon University, Pittsburgh, Pennsylvania 15213, Institute of Materials Science, NCSR "Demokritos", 15310 Ag. Paraskevi, Attiki, Greece, Departamento de Química, C.Q.F.B., Faculdade de Ciências e Tecnologia, Universidade Nova de Lisboa, Quinta da Torre, 2825-114 Caparica, Portugal, and Department of Physics, University of Ioannina, Ioannina, Greece

Received July 19, 2000

Abstract: Iron−sulfur clusters with [3Fe−4S] cores are widely distributed in biological systems. In the oxidized state, designated [3Fe−4S]$^{+}$, these electron-transfer agents have an electronic ground state with $S = {}^1/_2$, and they exhibit EPR signals centered at $g = 2.01$. It has been established by Mössbauer spectroscopy that the three iron sites of the cluster are high-spin Fe^{3+}, and the general properties of the $S = {}^1/_2$ ground state have been described with the exchange Hamiltonian $H_{exch} = J_{12}\mathbf{S}_1\cdot\mathbf{S}_2 + J_{23}\mathbf{S}_2\cdot\mathbf{S}_3 + J_{13}\mathbf{S}_1\cdot\mathbf{S}_3$. Some [3Fe−4S]$^{+}$ clusters (type 1) have their *g*-values confined to the range between $g = 2.03$ and 2.00 while others (type 2) exhibit a continuous distribution of *g*-values down to $g \approx 1.85$. Despite considerable efforts in various laboratories no model has emerged that explains the *g*-values of type 2 clusters. The 4.2 K spectra of all [3Fe−4S]$^{+}$ clusters have broad features which have been simulated in the past by using ^{57}Fe magnetic hyperfine tensors with anisotropies that are unusually large for high-spin ferric sites. It is proposed here that antisymmetric exchange, $H_{AS} = \mathbf{d}\cdot(\mathbf{S}_1 \times \mathbf{S}_2 + \mathbf{S}_2 \times \mathbf{S}_3 + \mathbf{S}_3 \times \mathbf{S}_1)$, is the cause of the *g*-value shifts in type 2 clusters. We have been able to fit the EPR and Mössbauer spectra of the 3Fe clusters of beef heart aconitase and *Desulfovibrio gigas* ferredoxin II by using antisymmetric exchange in combination with distributed exchange coupling constants J_{12}, J_{13}, and J_{23} (*J*-strain). While antisymmetric exchange is negligible for aconitase (which has a type 1 cluster), fits of the ferredoxin II spectra require $|d| \approx 0.4$ cm^{-1}. Our studies show that the data of both proteins can be fit using the same isotropic ^{57}Fe magnetic hyperfine coupling constant for the three cluster sites, namely $a = -18.0$ MHz for aconitase and $a = -18.5$ MHz for the *D. gigas* ferredoxin. The effects of antisymmetric exchange and *J*-strain on the Mössbauer and EPR spectra are discussed.

Introduction

Clusters with [3Fe−4S] cores are found in simple ferredoxins or more complex proteins such as the so-called 7Fe ferredoxins, NiFe hydrogenases, glutamate synthase, succinate dehydrogenase, and nitrite reductase.[1] Discovered by Mössbauer studies of the 7Fe ferredoxin from *Azotobacter vinelandii*,[2] the clusters were soon shown by chemical analyses, [3Fe] to [4Fe−4S] cluster conversions and spectroscopic studies to contain a cuboidal [3Fe−4S] core. High-resolution X-ray structures have been published for a variety of [3Fe−4S] cluster-containing proteins, among them *Desulfovibrio gigas (Dg)* ferredoxin II (FdII) and beef heart aconitase, the proteins of interest in the present work.[3,4] A recent review by Johnson, Duderstadt, and Duin[5] gives comprehensive data on many systems containing this cluster type. [3Fe−4S] clusters have been studied extensively in two oxidation states, namely the oxidized $S = {}^1/_2$ [3Fe−4S]$^{+}$ form and the reduced $S = 2$ [3Fe−4S]^{0} state. In this report we will be concerned with the electronic structure of the oxidized form, which we will designate for brevity as 3Fe cluster.

A variety of spectroscopic techniques have been applied to investigate the electronic structure of 3Fe clusters. Of particular relevance for the present study are EPR,[6−9] Mössbauer,[10−14]

* To whom correspondence should be addressed: Telephone: (412) 268-5058. Fax: (412) 268-1061. E-mail: em40@andrew.cmu.edu.
[†] Carnegie Mellon University.
[‡] Institute of Materials Science.
[§] Universidade Nova de Lisboa.
[||] University of Ioannina.

(1) (a) Beinert, H.; Holm, R. H.; Münck, E. *Science* **1997**, *277*, 653−659. (b) Johnson M. K. In *Encyclopedia of Inorganic Chemistry*; King, R. B., Ed.; Wiley: Chichester, 1994; Vol 4., pp 1896−1915. (c) Cammack, R. *Adv Inorg. Chem.* **1992**, *38*, 281−322. (d) *Iron Sulfur Proteins;* Lovenberg, W., Ed.; Academic Press: New York, 1973; Vols. I and II. (e) *Iron Sulfur Proteins;* Lovenberg, W., Ed.; Academic Press: New York, 1977; Vol III. (f) *Iron Sulfur Proteins*; Spiro, T. G., Ed.; Wiley: New York, 1982.

(2) Emptage, M. H.; Kent, T. A.; Huynh, B. H.; Rawlings, J.; Orme-Johnson, W. H.; Münck, E. *J. Biol. Chem.* **1979**, *255*, 1793−1796.

(3) Kissinger, C. R.; Sieker, L. C.; Adman, E. T.; Jensen, L. H. *J. Mol. Biol.* **1991**, *219*, 693−715.

(4) Robbins, A. H.; Stout, C. D. *Proc. Natl. Acad. Sci. U.S.A.* **1989**, *86*, 3639−3643.

(5) Johnson, M. K.; Duderstadt, R. E.; Duin, E. C. *Adv. Inorg. Chem.* **1999**, *47*, 1−82.

(6) (a) Gayda, J.-P.; Bertrand, P.; Guigliarelli, B.; Meyer, J. *J. Chem. Phys.* **1983**, *79*, 5732−5733. (b) Guigliarelli. B.; More, C.; Bertrand, P.; Gayda, J. P. *J.Chem. Phys.* **1986**, *85*, 2774−2778. (c) Guigliarelli, B.; Gayda, J. P.; Bertrand, P.; More, C. *Biochim. Biophys. Acta* **1986**, *871*, 149−155.

(7) Telser, J.; Lee, H.-I.; Hoffman, B. M. *J. Biol. Inorg. Chem.* **2000**, *5*, 369−380.

(8) Duderstadt, R. E.; Staples, C. R.; Brereton, P. S.; Adams, M. W. W.; Johnson M. K. *Biochemistry* **1999**, *38*, 10585−10593.

(9) Ruzicka, F. J.; Beinert, H. *J. Biol. Chem.* **1978**, *253*, 2514−2516.

(10) Surerus, K. K.; Kennedy M. C.; Beinert, H.; Münck, E. *Proc. Natl. Acad. Sci. U.S.A.* **1989**, *86*, 9846−9850.

10.1021/ja002658i CCC: $19.00
Published on Web 11/17/2000

ENDOR,[15] and NMR[12,16−18] results. EPR studies have revealed an $S = {}^1/_2$ ground state with features centered around $g = 2.01$; for a compilation of EPR data from various proteins see for instance refs 5−7. Mössbauer studies of a variety of 3Fe cluster-containing proteins have established that the clusters, in their oxidized state, contain three antiferromagnetically coupled high-spin Fe^{3+} sites. The general features of the observed ^{57}Fe magnetic hyperfine interactions were explained by the spin-coupling of Kent et al.[19] In this model three high-spin ferric sites ($S_1 = S_2 = S_3 = {}^5/_2$) are coupled by isotropic exchange interactions,

$$H = J_{12}\mathbf{S}_1\cdot\mathbf{S}_2 + J_{23}\mathbf{S}_2\cdot\mathbf{S}_3 + J_{13}\mathbf{S}_1\cdot\mathbf{S}_3 \qquad (1)$$

For $J_{ij} > 0$ and roughly equal J_{ij} (see ref 19) the coupled system produces two low-lying $S = {}^1/_2$ multiplets whose energy difference, δ, depends on differences between the J_{ij} (see eq 5 below). The next group of excited states in the spin ladder of oxidized 3Fe clusters are four multiplets with $S = {}^3/_2$, centered at energy $3J/2$. Recent studies of the spin−lattice relaxation rates[7,20] have shown that the J_{ij} are the same ($J_{12} \approx J_{13} \approx J_{23} = J$) within 10 cm^{-1}. Low-temperature magnetic susceptibility[21] and room-temperature NMR studies of *Dg* FdII[17] have established that the J_{ij} are larger than 200 cm^{-1}; $J > 200$ cm^{-1} by magnetic susceptibility and $J \approx 300$ cm^{-1} by NMR. J_{ij} values around 300 cm^{-1} are also compatible with room-temperature NMR studies of the ferredoxins from *Pyrococcus furiosus (Pf* Fd)[18a] and *Rhodopseudomonas palustris*.[22]

While the general features of the spin structure of 3Fe clusters are well understood, some conspicuous features of the EPR and Mössbauer spectra have not been explained. First, the EPR spectra of most 3Fe clusters exhibit broad tails at the high-field end. This broadening is particularly evident for *Dg* FdII, *Pf* Fd, and a ferredoxin from *Desulfovibrio africanus*.[6] Second, because the constituent Fe sites are high-spin ferric, isotropic ^{57}Fe magnetic hyperfine interactions, $A_i\mathbf{S}_i\cdot\mathbf{I}_i$, are expected. However, the Mössbauer spectra of all 3Fe clusters, in particular those of *Dg* FdII and *Pf* Fd, have broad features that cannot be simulated with (nondistributed) isotropic hyperfine fields. To simulate these spectra we[10−12,14] and others[13] have used anisotropic **A**-tensors (anisotropic *A*-values produce orientation-depended magnetic splittings and thus broaden the spectra). While some anisotropies have been observed for the high-spin ferric sites in rubredoxin (anisotropy < 3%) and in $[2Fe\text{-}2S]^{1+}$ clusters (typically $A_x \approx -53$ MHz, $A_y \approx -48$ MHz, $A_z \approx -43$ MHz),[23] it was evident that the isotropic coupling model of Kent et al. had to be amended by terms capable of describing the peculiar features observed by EPR and Mössbauer spectroscopy. The unusual properties of 3Fe clusters are also evident in their ENDOR spectra. Thus, well-defined ^{57}Fe ENDOR resonances were observed at $g \approx 2.02$ but signals were difficult to detect when the EPR was tuned to *g*-values below $g = 2.00$.[15]

To explain the unusual EPR spectra of 3Fe clusters Bertrand and co-workers have considered mixing of excited $S = {}^3/_2$ states with the $S = {}^1/_2$ ground state by zero-field splitting (ZFS) interactions, $\sum S_i\cdot D_i\cdot S_i$, of the local ferric sites (D/J mixing). Because the ZFS interactions are anisotropic, such mixing can produce the desired anisotropic Zeeman interactions. By assuming that the ZFS parameters are distributed about their mean values, these authors were able to produce very good fits to the EPR spectra for a variety of 3Fe ferredoxins.[6] However, the fits required that $D_i/J \approx 0.05$ for *Dg* FdII and because the intrinsic D_i values of tetrahedral $Fe^{3+}S_4$ sites are ~ 2 cm^{-1}, *J*-values of about 40 cm^{-1} were anticipated from the mixing model. When the subsequent magnetic susceptibility[21] and NMR studies[17] of *Dg* FdII showed that the J_{ij} were substantially larger, it became clear that D/J mixing could not explain the experimental data.

One interaction, rarely considered in the literature, that can produce anisotropic Zeeman interactions in Fe^{3+}-containing clusters is antisymmetric (Dzyaloshinskii−Moriya) exchange. Antisymmetric exchange between two spins $\mathbf{S_1}$ and $\mathbf{S}_2$ can be written as $\mathbf{S}_1\cdot\mathbf{J}_{AS}\cdot\mathbf{S}_2$ where $\mathbf{J}_{AS}$ is an antisymmetric tensor. Alternatively, this interaction can be written as $\mathbf{d}_{12}\cdot\mathbf{S}_1 \times \mathbf{S}_2$ where $\mathbf{d}_{12}$ is pseudovector. For three Fe pairs this interaction becomes $\boldsymbol{H}_{AS} = \mathbf{d}_{12}\cdot\mathbf{S}_1 \times \mathbf{S}_2 + \mathbf{d}_{23}\cdot\mathbf{S}_2 \times \mathbf{S}_3 + \mathbf{d}_{31}\cdot\mathbf{S}_3 \times \mathbf{S}_1$. As long as mixing with the $S = {}^3/_2$ states is negligible, the three pseudovectors $\mathbf{d}_{ij}$ can be combined into one,[24] with the result that the antisymmetric exchange term can be written as

$$H_{AS} = \mathbf{d}\cdot(\mathbf{S}_1 \times \mathbf{S}_2 + \mathbf{S}_2 \times \mathbf{S}_3 + \mathbf{S}_3 \times \mathbf{S}_1) \qquad (2)$$

Tsukerblat and co-workers[24] have studied extensively the consequences of $H = H_{exch} + H_{AS}$ on the electronic properties of trinuclear clusters. In particular the paper by Fainzil'berg, Belinskii, and Tsukerblat[25] provides an incisive theoretical analysis of EPR and Mössbauer properties that derive from the combined eqs 1 and 2 for $J_{13} = J_{23}$. These workers, as well as Rakitin et al.,[26] have shown that antisymmetric exchange in trinuclear iron clusters can lower the *g*-values of the $S = {}^1/_2$ ground doublet by mixing of the two $S = {}^1/_2$ states that occur in the coupled system. Using Mössbauer spectroscopy we have recently studied antisymmetric exchange in the antiferromagnetically coupled diiron cluster of methane monooxygenase and a synthetic complex.[27] These studies yielded surprisingly large values for *d*, namely $d \approx 2.2$ cm^{-1} and $d = 1.5$ cm^{-1},

(11) Hu, Z.; Jollie, D.; Burgess, B. K.; Stephens, P. J.; Münck, E. *Biochemistry* **1994**, *33*, 14475−14485.
(12) Macedo, A. L.; Moura, I.; Surerus, K. K.; Papaefthymiou, V.; Liu, M.-Y.; LeGall, J.; Münck, E.; Moura, J. J. G. *J. Biol. Chem.* **1994**, *269*, 8052−8058.
(13) Huynh, B. H.; Patil, D. S.; Moura.; I, Teixeira, M.; Moura. J. J. G.; DerVartanian, D. V.; Czechowski, M. H.; Prickril, B. C.; Peck, H. D., Jr.; LeGall, J. *J. Biol. Chem.* **1987**, *262*, 795−800.
(14) Surerus, K. K.; Chen, M.; van der Zwaan, W.; Rusnak, F. M.; Kolk, M.; Duin, E. C.; Albracht, S. P. J.; Münck, E. *Biochemistry* **1994**, *33*, 4980−4993.
(15) (a) Fan, C.; Houseman, A. L. P.; Doan, P.; Hoffman, B. M. *J. Phys. Chem.* **1993**, *97*, 3017−3022. (b) Fu, W.; Telser, J.; Hoffman, B. M.; Smith E. T.; Adams, M. W. W.; Finnegan, M. G.; Conover, R. C.; Johnson, M. K. *J. Am. Chem. Soc.* **1994**, *116*, 5722−5729. (c) Telser, J.; Huang, H.; Lee, H.-I.; Adams, M. W. W.; Hoffman, B. M. *J. Am. Chem. Soc.* **1998**, *120*, 861−870.
(16) Bertini, I.; Ciurli, S.; Luchinat, C. *Struct Bonding* **1995**, *83*, 1−54.
(17) Macedo, A. L.; Moura, I.; Moura, J. J. G.; Le Gall, J.; Huynh, B. H. *Inorg. Chem.* **1993**, *32*, 2, 1101−1105.
(18) (a) Busse, S. C.; La Mar, G. N.; Yu, L. P.; Howard, J. B.; Smith, E. T.; Zhou, Z. H.; Adams, M. W. W. *Biochemistry* **1992**, *31*, 11952−11962. (b) Gorst, C. M.; Yeh, Y.-H.; Teng, Q.; Calzolai, L.; Zhou, Z.-H.; Adams, M. W. W.; La Mar, G. N. *Biochemistry* **1995**, *34*, 4, 600−610.
(19) Kent, T. A.; Huynh, B. H.; Münck, E. *Proc. Natl. Acad. Sci. U.S.A.* **1980**, *77*, 6574−6576.
(20) Hung, S.-C.; Grant, C. V.; Peloquin, J. M.; Waldeck, A. R.; Britt, R. D.; Chan, S. I. *J. Phys. Chem. A* **2000**, *104*, 4402−4412.
(21) Day, E. P.; Peterson, J.; Bonvoisin, J. J.; Moura, I.; Moura, J. J. G. *J. Biol. Chem.* **1988**, *263*, 3684−3689.
(22) Bertini, I.; Dikiy, A.; Luchinat, C.; Macinai, R.; Viezzoli, M. S.; Vincenzini, M. *Biochemistry* **1997**, *36*, 3570−3579.
(23) Sands, R. H.; Dunham, W. R. *Q. Rev. Biophys.* **1975**, *7*, 443−504.
(24) Tsukerblat, B. S.; Belinskii, M. I.; Fainzil'berg, V. I. *Sov. Sci. Rev., Sect. B.* **1987**, *9*, 337−481.
(25) Fainzil'berg, V. I.; Belinskii, M. I.; Tsukerblat, B. S. *Mol. Phys.* **1981**, *44*, 1195−1213.
(26) Rakitin, Y. V.; Yablokov, Y. V.; Zelentsov, V. V. *J. Magn. Res.* **1981**, *43*, 288−301.
(27) Kauffmann, K. E.; Popescu, C. V.; Dong, Y.; Lipscomb, J. D.; Que, L., Jr.; Münck, E. *J. Am. Chem. Soc.* **1998**, *120*, 8739−8746.

respectively. These values, however, are similar to $d = 1.4$ cm^{-1} reported from EPR analysis of trinuclear iron acetate.[26] If 3Fe clusters containing ferric FeS_4 sites would exhibit d values around 0.5 cm^{-1}, antiferromagnetic exchange could produce g-values in the range observed for 3Fe clusters.

In the present report we present evidence that antisymmeric exchange in combination with narrowly distributed J_{ij} values can account for the features of the EPR and Mössbauer spectra of 3Fe clusters of *Dg* Fd II. We will also show that the Mössbauer spectra of aconitase and *Dg* FdII can be fitted using the same isotropic magnetic hyperfine coupling constant for each iron site.

Materials and Methods

Dg FdII was purified as previously described.[17,28] Samples were prepared in 10 mM phosphate buffer, pH 7.6.

EPR spectra were recorded on a Bruker ESP 300 equipped with an ESR 910 helium continuous-flow cryostat and an Oxford temperature controller.

For the interpretation of the EPR spectra of Figure 7 we have used a program written by Dr. M. P. Hendrich of Carnegie Mellon University. We have used a line width tensor in g-space with Gaussian width $\sigma_{gx} = \sigma_{gy} = 0.01$ and $\sigma_{gz} = 0$. This tensor was used to compute for each orientation of the magnetic field, $B(\Theta,\Phi)$, a σ-value in B-space, $\sigma_g(\Theta,\Phi)$. To this was added a fixed width in B-space, σ_B, to obtain $\sigma = \sqrt{\sigma_g^2(\Theta,\Phi)+\sigma_B^2}$. The width at $B(\Theta,\Phi)$ was thus a Gaussian of width σ.

Theoretical Background

The principal features of oxidized 3Fe clusters are well described by the Heisenberg−Dirac−vanVleck exchange Hamiltonian of eq 1. NMR, susceptibility, EPR, and Mössbauer studies have shown that the $J_{ij} > 200$ cm^{-1} and that the three J_{ij}-values are equal to within 3%. Without loss of generality we assume that $J_{23} \geq J_{12} \geq J_{13}$. For $S_1 = S_2 = S_3 = {}^5/_2$ two configurations with $S = {}^1/_2$ occur in the coupled system. These may be obtained by coupling $\mathbf{S}_2$ and $\mathbf{S}_3$ to an intermediate spin $S_{23} = 2$ or 3, and then coupling $\mathbf{S_{23}}$ to $\mathbf{S_1}$ to obtain the system spin $\mathbf{S}$. Using the nomenclature $|S_{23},S_1;S,M\rangle$, the two doublets with $S = {}^1/_2$ have the form

$$|^2\mathbf{1}, M\rangle = (1-\alpha^2)^{1/2}\,|2,{}^5/_2;{}^1/_2,M\rangle + \alpha|3,{}^5/_2;{}^1/_2,M\rangle \qquad (3)$$

$$|^2\mathbf{2}, M\rangle = -\alpha|2,{}^5/_2;\,{}^1/_2,M\rangle + (1-\alpha^2)^{1/2}\,|3,{}^5/_2;{}^1/_2,M\rangle \qquad (4)$$

where α is the mixing parameter given by Kent et al. as

$$\alpha^2 = {}^1/_2(1 - 1/\sqrt{1+x^2})$$

with

$$x = \sqrt{3}\frac{J_{12}-J_{13}}{2J_{23}-J_{12}-J_{13}}$$

The values $J_{13} = J_{12} \neq J_{23}$ yield $\alpha = 0$ and $|2,{}^5/_2;{}^1/_2,M\rangle$ is the ground state. This doublet is separated by $\delta = 3(J_{23} - J_{13})$ from the excited $|3,{}^5/_2;{}^1/_2,M\rangle$ doublet. The other extreme occurs for $J_{12} = J_{23} \neq J_{13}$, giving $\alpha^2 = 0.25$; all solutions are described by $0 \leq \alpha \leq 1/4$.[19] The energy splitting, δ, between the two doublets depends on the difference between the J-values and is given by

$$\delta = 3(J_{23} - J_{13})\sqrt{1-\omega+\omega^2} \qquad (5)$$

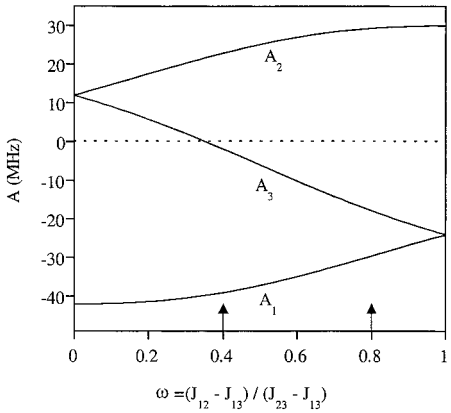

Figure 1. Effective A-values for sites 1, 2 and 3 calculated as a function of ω using $a(^{57}\text{Fe}) = -18$ MHz for the local magnetic hyperfine coupling constants. The right and left arrows indicate the average ω-values used to calculate the Mössbauer spectra of aconitase and *Dg* FdII, respectively. The labeling of the three sites follows from the choice $J_{23} > J_{12} > J_{13}$.

with $\omega = (J_{12} - J_{13})/(J_{23} - J_{13})$ and $0 \leq \omega \leq 1$. Electron spin−lattice relaxation studies of Telser et al.[7] have shown that $\delta = 13$ cm^{-1} for the 3Fe cluster of aconitase and $\delta = 26$ cm^{-1} for *Dg* FdII. By estimating the inequivalence of the exchange coupling constants from magnetic hyperfine interactions obtained by Mössbauer and ENDOR spectroscopy, these authors have also estimated that $J_{23} - J_{13} \approx 5$ cm^{-1} for aconitase and ≈ 10 cm^{-1} for *Dg* FdII. These values constrain the permissible differences of the J-values in eq 5.

To describe the Zeeman interactions and the ^{57}Fe magnetic hyperfine interactions we augment the Hamiltonian of eq 1 by

$$H_{\text{Zeeman}} = \sum_i \beta \mathbf{S}_i \cdot \mathbf{g}_i \cdot \mathbf{B} \qquad (6)$$

$$H_{\text{hf}} = \sum_i (\mathbf{S}_i \cdot \mathbf{a}_i \cdot \mathbf{I}_i - g_n \beta_n \mathbf{B} \cdot \mathbf{I}_i) \qquad (7)$$

where g_i and a_i refer to the individual sites ($i = 1, 2, 3$). EPR[29] and Mössbauer[30] studies of monomeric ferric FeS_4 sites sites have shown that g_i and $\boldsymbol{a_i}$ are isotropic to within 1 and 3%, respectively. Using the Wigner−Eckart theorem, we can replace the operators of the site spins in eqs 5 and 6 by the operator of the system spin

$$H_{\text{Zeeman}} = \beta \mathbf{S} \cdot \mathbf{g} \cdot \mathbf{B} \qquad (8)$$

$$H_{\text{hf}} = \sum_i \mathbf{S} \cdot \mathbf{A}_i \cdot \mathbf{I}_i - g_n \beta \mathbf{B} \cdot \mathbf{I}_i \qquad (9)$$

with

$$\mathbf{g} = \sum_i K_i \cdot \mathbf{g}_i \qquad (10)$$

$$\mathbf{A}_i = K_i \cdot \mathbf{a}_i \qquad (11)$$

$K_i = 2\,\langle^2\mathbf{1}|S_{iz}|^2\mathbf{1}\rangle$ are the spin projection factors. Figure 1 shows the dependence of the effective A-values, or alternatively the spin projection factors, as J_{12} is varied between J_{13} and J_{23}. The

(28) Bruschi, M.; Hatchikian, C. E.; LeGall, J.; Moura, J. J. G.; Xavier, A. V. *Biochim. Biophys. Acta* **1976**, *449*, 275−284.

(29) (a) Gebhard, M. S.; Deaton, J. C.; Koch, S. A.; Millar, M.; Solomon, E. I. *J. Am. Chem. Soc.* **1990**, *112*, 2217−2231. (b) Brandt, G.; Räuber, A.; Schneider, J. *Solid State Commun.* **1973**, *12*, 481−483. (c) Sweeney, W. V.; Coffman, R. E. *Biochim. Biophys. Acta* **1972**, *286*, 26−35.

(30) (a)Schulz, C.; Debrunner, P. G. *J. Phys.* **1976**, *C6−37*, 153−158. (b)Moura, I.; Huynh, B. H.; Hausinger, R.; LeGall, J.; Xavier, A. V.; Münck, E. *J. Biol. Chem.* **1980**, *255*, 2493−2498.

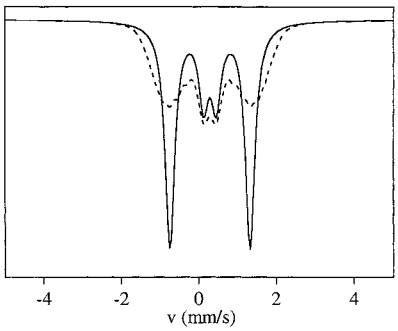

Figure 2. Mössbauer spectra illustrating the effect of a distributed J_{12}. Spectra, corresponding to site 3 of the 3Fe cluster of aconitase, were calculated for a $= -18$ MHz, $J_{13} = 300$ cm^{-1}, $J_{23} = 305$ cm^{-1}. Solid line: $J_{12} = 304$ cm^{-1}. Dashed: $J_{12} = 304$ cm^{-1} distributed with Gaussian $\sigma = 1$ cm^{-1}. Spectral areas are normalized.

effective *A*-values can be very sensitive to small variations of the *J*-values. For instance, minor variations of J_{12} around its mean value can lead to considerable broadening of the Mössbauer spectra. This broadening is illustrated in Figure 2 which shows theoretical spectra for site 3 of the aconitase cluster for fixed $J_{13} = 300$ cm^{-1}, $J_{23} = 305$ cm^{-1} and $J_{12} = 304$ cm^{-1} (solid lines) and for the case where J_{12} has a Gaussian distribution (dashed) with $\sigma_{J12} = 1$ cm^{-1} centered around $J_{12} = 304$ cm^{-1}. The broadening introduced by the distributed J_{12} can easily be mistaken for the presence of anisotropic magnetic hyperfine interactions, especially when the spectral contributions of the three sites overlap.

The principal *g*-values of Fe^{3+} ions with tetrahedral sulfur coordination have been found to be confined to values between 2.016 and 2.033.[29] By using these extremes in eq 10 and orienting the **g**-tensors of the individual sites such as to produce maximal anisotropy of **g**, one finds that the *g*-values of the system should be confined the range between 1.99 and 2.05. The *g*-values of about a dozen 3Fe clusters have been reported, and for *Pf* Fd the EPR spectra of six mutants have been studied; see Table 5 and Figure 4 of ref 5 (The mentioned variants involve mutations of the proximal aspartate ligand; this ligand coordinates to the fourth Fe site in the [4Fe−4S] form of the ferredoxin). These studies have revealed that the largest *g*-value is confined to the narrow range between 2.018 and 2.032. The smallest *g*-values, however, were found to be as low as 1.70. Clearly, an explanation of the unusual *g*-values of the 3Fe clusters requires an additional term in the electronic spin Hamiltonian. In the following we will argue that antisymmetric exchange can provide the desired correction.[31]

The antisymmetric exchange term of eq 2 will mix the two $S = {}^1/_2$ doublets, ^{2}**1** and ^{2}**2**. Because the interactions in eq 1 and 6 are isotropic, the AS exchange term introduces the only physically distinct direction into the electronic Hamiltonian. Without loss of generality we call the direction of **d** the *z*-direction, $d_z = d$, and thus the antisymmetric interactions between the three Fe sites are described by one parameter. Because the g_i in eq 6 are expected to be isotropic to within 1%, we will treat them as a scalar g_0.

The Hamiltonian

$$H = H_{\text{exch}} + \sum_i g_0 \beta \mathbf{S}_i \cdot \mathbf{B} + H_{\text{AS}} \tag{12}$$

splits the two $S = {}^1/_2$ doublets by (see eq 5)

$$\Delta = \sqrt{\delta^2 + 243 d^2} \tag{13}$$

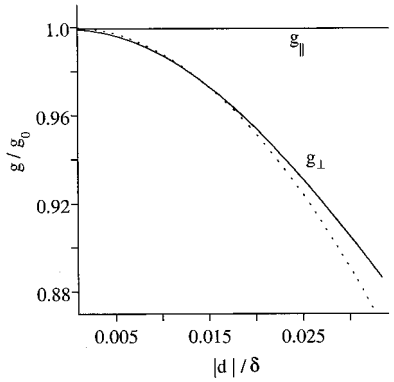

Figure 3. Effective *g*-values for the $S = {}^1/_2$ ground doublet as a function of d/δ according to the expression of eq 14 (dashed line) and according to the exact expression[25,26] (solid line). δ is defined in eq 5.

in zero field and, in the limit $|d|, \beta B \ll \delta$, the effective *g*-values of the ground doublet (Figure 3) are[25,26]

$$g_{\|} = g_0 \quad g_{\perp} = g_0\left(1 - \frac{243}{2}\frac{d^2}{\delta^2}\right) \tag{14}$$

It is important to note that the AS exchange term produces axial EPR spectra with $g_\perp < g_{\|}$. Equation 14 yields for $|d|/\delta = 0.02$ *g*-values as low as 1.90. For $|d|/\delta$ values as small as 0.02 the energy splittings measured by Telser et al. are essentially a measure of δ, that is, $\delta \approx \Delta$. For the following discussion of the EPR and Mössbauer spectra of 3Fe clusters the reader may take as a guide that the three J_{ij} values differ by less than 10 cm^{-1}, that $J_{ij} \approx 300$ cm, and that $|d| \leq 0.5$ cm^{-1}.

The effects of antisymmetric exchange on the Mössbauer spectra are very different for the three Fe sites of the cluster. For $d = 0$ and isotropic a_i the internal magnetic fields measured by Mössbauer spectroscopy, $\mathbf{B}_{\text{int}}(i) = -a_i \langle \mathbf{S_i} \rangle / g_n \beta_n$, are collinear with the applied field **B** (The $\langle S_i \rangle$ can be obtained from Figure 1 by dividing the A_i-values by $2a_i = -36$ MHz). For $d \neq 0$ and for **B** parallel to **d** the magnitude of $\mathbf{B_{int}}$ is modified, but the internal field is still collinear to **B**. For applied fields perpendicular to **d** the internal field acquires a component perpendicular both to **B** and **d** (this is the effect of the cross terms in eq 2). The parallel component has a contribution proportional to $\langle S_i \rangle$ and a contribution proportional to d^2/δ^2. The transverse component is proportional to d/δ.[25] As shown in Figure 1 the spin expectation value $\langle S_{z3} \rangle$ can be small or zero (for $\omega = 0.35$). Under these circumstances the magnetic splitting is dominated by H_{AS}. This is illustrated in Figure 4A which shows $B = 0.06$ T spectra generated for $d/\delta = 0.02$ (dashed) and for $d/\delta = 0$. In an applied field of 6.0 T the antisymmetric contribution is dominated by the nuclear Zeeman term, and the spectra become quite insensitive to *d*.

For the analysis of the Mössbauer spectra we have written a computer program that computes spectra from

$$H = H_{\text{exch}} + H_{\text{AS}} + H_{\text{Zeeman}} + H_{\text{hf}} + H_Q \tag{15}$$

$$H_Q = \sum_i \frac{eQV_{zz}(i)}{12}\{3\mathbf{I}_z^2(i) - {}^5/_4 + \eta[\mathbf{I}_x^2(i) - \mathbf{I}_y^2(i)]\} \tag{16}$$

where *i* sums over the three sites. Equation 16 describes the quadrupole interactions of the three Fe sites; $\eta = (V_{xx} - V_{yy})/$

(31) Guigliarelli and Bertrand[32] have suggested in a recent review article that antisymmetric exchange can mix the two $S = {}^1/_2$ states and that such mixing should be explored by a quantitative model.

(32) Guigliarelli, B.; Bertrand, P. *Adv. Inorg. Chem.* **1999**, *47*, 421−497.

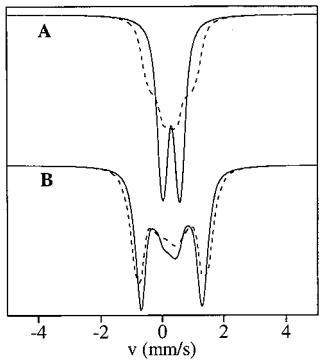

Figure 4. Calculated Mössbauer spectra illustrating the effects of antisymmetric exchange. The spectra correspond to those of site 3 of *Dg* FdII for $J_{13} = 300$ cm^{-1}, $J_{23} = 310$ cm^{-1}, $J_{12} = 304$ cm^{-1}, $a_3 = -18.5$ MHz, $\Delta E_Q = 0.52$ mm/s and $\eta = 0$. Parallel field 0.06 T spectra (A) and 6.0 T spectra (B) were computed for $d = 0$ (solid lines) and $d = 0.6$ cm^{-1} (dashed).

V_{zz} is the asymmetry parameter. The three electric field gradient (EFG) tensors of a [3Fe−4S] cluster are expected to have different principal axis systems. However, the EFG-tensors of the three sites are small, and the spectra are quite insensitive to details of the quadrupole interactions. Therefore, we have kept the three EFG-tensors collinear in our simulations.

We have solved eq 15 by diagonalizing the matrices of the whole system in the coupled representation $|S_{23},S_1;S,M\rangle$. Choosing the coupled representation allowed us to explore mixing of the multiplets by zero-field splitting and antisymmetric exchange terms and truncate the system later by retaining only the configurations that mattered, namely the two $S = {}^1/_2$ multiplets.

Results

Aconitase. The EPR spectra of the 3Fe cluster of aconitase are quite sharp and confined to a very narrow range of *g*-values; see for instance Beinert and Ruzicka[9] and Telser et al.[7] We have obtained very good simulations to an X-band spectrum[33] for $g_z = 2.029$, $g_y = 2.022$, and $g_x = 2.006$ by assuming that the *g*-values are distributed (*g*-strain) with Gaussian widths $\sigma_{gz} = 0.0035$, $\sigma_{gy} = 0.005$, and $\sigma_{gx} = 0.005$. The *g*-values differ slightly (<0.005) from those obtained at Q-band by Telser et al.;[7] however, it should be noted that the samples were from different preparations and that the spectrometers used different detection modes. Since all *g*-values of aconitase are above $g = 2.00$, we see no need to consider antisymmetric exchange for the aconitase cluster.

Mössbauer spectra (4.2 K) of aconitase are shown in Figure 5. These spectra were fitted by Surerus and co-workers[10] with an isotropic *A*-value of +21.1 MHz for site 2. However, the spectra of site 1 were simulated with an **A**-tensor that had 10% anisotropy, and more to the point, a fit to the spectra of site 3 required an **A**-tensor of considerable anisotropy, namely $A_x(3) = -2.3$ MHz, $A_y(3) = -21.9$ MHz, and $A_z(3) = -7.4$ MHz. As pointed out above, such a large anisotropy is unprecedented for a high-spin ferric ion, and therefore we and others have searched for a more physical explanation of the broad spectral features. Inspection of Figure 1 reveals that an explanation for

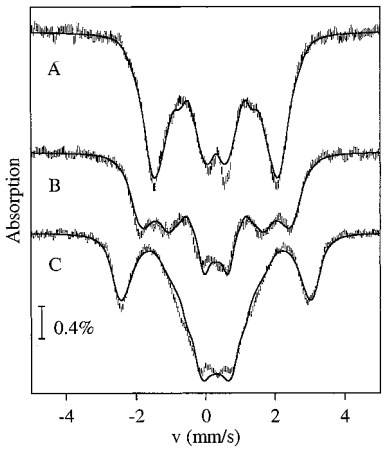

Figure 5. Mössbauer spectra of the [3Fe−4S]$^+$ cluster of aconitase recorded at 4.2 K in parallel applied fields of 0.06 T (A), 2.5 T (B), and 6.0 T; same spectra as those reported previously.[10] Solid lines are theoretical spectra computed for $a_1 = a_2 = a_3 = -18$ MHz using $J_{13} = 300$ cm^{-1}, $J_{23} = 305$ cm^{-1}, and $J_{12} = 301.5$ (4%), 302.5 (21%), 303.5 (30%), 304.5 (34%), and 305 cm^{-1} (11%); the numbers in parentheses give percentages of the subcomponent in the summed spectra. For the quadrupole splittings we used $\Delta E_Q = 0.73$ mm/s and $\eta = 1$ for all sites.

the broad features observed for sites 1 and 3 can be obtained by assuming that the J_{ij}-values are distributed about their mean values, and keeping all *a*-values isotropic.[34] The value $\delta = 13$ cm^{-1} reported by Telser and co-workers indicates, eq 5, that the J_{ij} differ by about 5 cm^{-1}. For the considerations below only the differences between the J_{ij}-values matter but not their absolute values. Therefore, and taking into account the results of magnetic susceptibility and NMR studies, we will quite arbitrarily choose for the lowest *J*-value, $J_{13} = 300$ cm^{-1}.

Inspection of the graph in Figure 1 shows that one can significantly broaden the spectra of sites 1 and 3 by choosing $J_{13} = 300$ cm^{-1}, $J_{23} = 305$ cm^{-1} and distributing J_{12} over the very narrow range of 2−3 cm^{-1} centered at 304 cm^{-1} ($\omega = 0.8$, see right arrow in Figure 1). We have therefore explored whether the Mössbauer spectra of aconitase can be fitted by assuming that all three Fe sites have the same local isotropic magnetic hyperfine coupling constants, $a_1 = a_2 = a_3$. There is nothing special about J_{12}, except that A_1 and A_3 are more sensitive to variations of J_{12}. Of course, a distributed J_{12} would suggest that the other two *J*-values are distributed as well. However, the spectra of the three sites are not well enough resolved to discriminate between individual variations of the three *J*-values. Therefore, we have confined our analysis to variations of J_{12} alone.

To analyze the data of Figure 5 we have chosen $J_{13} = 300$ cm^{-1}, $J_{23} = 305$ cm^{-1} and calculated spectra for 301 cm^{-1} ≤ J_{12} ≤ 305 cm^{-1} at 0.5 cm^{-1} intervals. We have then tested whether the data could be explained by assuming that J_{12} has a Gaussian distribution. This assumption, however, produced poor fits to the spectra. We have therefore used a least-squares fitting routine to determine the fractional populations that best represent the entire data set. Our simulations revealed that spacing the grid of J_{12} values in 1 cm^{-1} intervals produced rather satisfactory representations of the data. The theoretical curves drawn through the data of Figure 5 were obtained by summing spectra generated for different J_{12} values given in the caption. It is noteworthy that the spectra can be simulated very well by assuming the same, and isotropic, magnetic hyperfine coupling constant for all three Fe sites, $a = -18$ MHz.

***Desulfovibrio gigas* FdII.** The EPR spectra of *Dg* FdII are

(33) The spectrum was recorded by K. K. Surerus in 1986 on sample provided by Drs. H. Beinert and M. C. Kennedy**.** The spectrum was recorded at 9.228 GHz and ≈ 8 K at a microwave power of 0.1 mW, with a modulation amplitude of 1 mT.

(34) While writing up the present work we were informed by Dr. B. H. Huynh of Emory University that Dr. C. Krebs in his laboratory has fitted the spectra of a type 1 3Fe cluster by using a distribution of *J*-values while keeping the **A**-tensors isotropic.

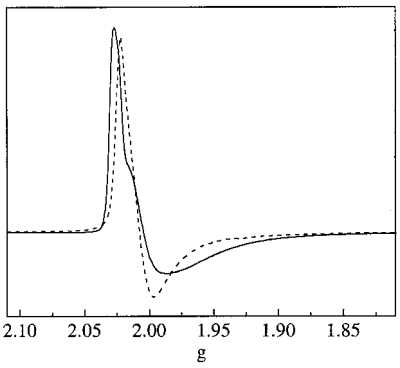

Figure 6. X-band EPR spectra of two preparations of *Dg*FdII recorded at ~8 K under nonsaturating conditions. The spectra of sample A (solid line) and B (dashed) were recorded on different instruments. Protein concentrations were ~0.8 mM. Sample A was obtained by reoxidation of a dithionite-reduced sample while sample B was obtained by aerobic purification of the protein. Conditions for sample A: 9.63 GHz, microwave power, 126 mW; modulation, 0.5 mT. Sample B: 9.65 GHz, 2 μW, 0.4 mT.

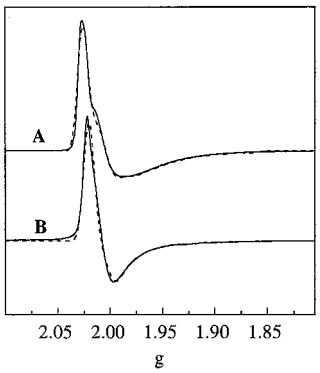

Figure 7. Spectral simulations (dashed) for *Dg* FdII samples A (top) and B (bottom) using axial spectra with $g_z > g_{perp}$ with the distributions of subspectra shown in Figure 8. For samples A and B we used $g_0 =$ 2.0027 and 2.0022, respectively. For line width parameters see Materials and Methods.

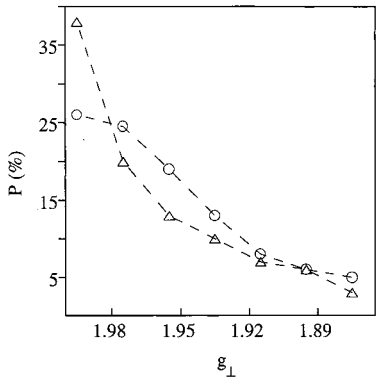

Figure 8. Distribution of subspectra used to generate the theoretical spectra shown in Figure 7. Circles refer to sample A and triangles to sample B.

substantially broader than those of aconitase. Comparison of the shapes of published spectra for this ferredoxin have revealed substantial variation in the shapes of the signal. We have made similar observations for our preparations. This is illustrated in Figure 6 which shows spectra from two preparations, sample A and B, of *Dg* FdII recorded under nonsaturating conditions. Note that the maximum *g*-value, $g_{||}$, differs by 0.005 between the samples and note the broader features of sample B (solid line) below $g = 2$. We have also observed small line shape changes after thawing and refreezing a sample. It is known that the *Dg* FdII cluster is very sensitive to perturbations of the protein structure. For instance, using NMR, EPR, and Mössbauer spectroscopy Macedo et al.[17] have shown that the oxidized 3Fe cluster exhibits two spectral forms, $FdII_{OX}$ and $FdII_{int}$, depending on whether cys-18 and cys-42, which are positioned ~12 Å from the 3Fe cluster, form a disulfide bridge or exist as thiolates, respectively. The FdII samples used in the present work were obtained either after aerobic purification of the protein or by exposure of a reduced sample to air at 4 °C for at least 12 h. After either procedure, $FdII_{int}$ will be absent. Given that the shapes of the FdII EPR spectra depend on the preparations in a way presently not understood, it is apparent that there is not one particular distribution of parameters that characterizes *Dg* FdII samples.

Telser et al.[7] as well Bertrand and co-workers[6b] have analyzed the EPR spectra of *Dg* FdII with a distributed set of *rhombic* *g*-values. The former group treated the three *g*-values as random variables while the latter used a model involving mixing of $S = {}^1/_2$ and $S = {}^3/_2$ by local zero-field splittings (D/J mixing). Because D/J-mixing involves the $S = {}^3/_2$ manifolds, the quantities D_i/J are too small to affect the *g*-values in a significant way (see Figure 1 of ref 6b for $D/J < 0.01$). As pointed out above, antisymmetric exchange mixes the two closely spaced $S = {}^1/_2$ manifolds and produces *axial* **g**-tensors given by the expression of eq 14. If antisymmetric exchange is indeed responsible for the observation of *g*-values below $g = 2.0$, one should be able to simulate the spectra of FdII with a distribution of *axial* **g**-tensors. If we ignore fine details such as minor rhombicities of the local **g**-tensors, it is the quantity d/δ that will control the *g*-values and their distribution. Because d/δ depends on *d*, and implicitly on J_{12}, J_{13}, and J_{23}, the distribution of at least four parameters can effect the EPR spectrum. The theoretical spectra shown Figure 7 (dashed) were obtained by simulating 14 axial spectra with fixed $g_{||}$ (see caption) and $g_\perp$ at 2.01, 2.00, 1.99...1.87. We then used a least-squares fitting program to determine the weights of the individual spectra in the distribution (Figure 8**)**. Telser et al.[7] suggest that the uncertainty in δ is $\pm$ 4 cm^{-1}. If we take these uncertainties as a guide and allow that the *d*-values are distributed between 0.3 and 0.5 cm^{-1}, the above range of $g_\perp$-values can be explained (The reader may also keep in mind that the reported δ-value must reflect an average over an unknown distribution.). From the fits shown in Figure 8 we conclude that the spectra of *Dg* FdII are compatible with a distribution of *axial* spectra.

Mössbauer spectra recorded at 4.2 K in parallel applied magnetic fields are shown in Figures 9 and 10. To give the reader an appreciation for the need of distributed parameters, we have plotted in Figure 9 a theoretical spectrum for $J_{13} =$ 300 cm^{-1}, $J_{12} = 304$ cm^{-1}, $J_{23} = 310$ cm^{-1}, and $d = 0$ assuming that each Fe site has an isotropic magnetic hyperfine coupling constant $a_i = -18.5$ MHz. Although the simulations give roughly the correct line positions for the spectra of the three sites, the broad features of the 60 mT spectrum of FdII are not properly represented by using isotropic *a*-values and fixed *J*-values.

The shape of the EPR spectrum of *Dg* FdII can be described by the distribution of one quantity, namely d/δ. The Mössbauer spectra, in contrast, depend in a complex way on the distributions of *d*, J_{12}, J_{13}, and J_{23}, as can be seen from the following argument. Consider, for instance, variations of the *J*-values. Suppose that J_{12} is close to J_{13}, that is, ω is close to zero. Inspection of Figure 1 reveals that a large variation of J_{23} is required to produce a substantial change of the effective *A*-values (Recall that the graph covers the entire range of possible

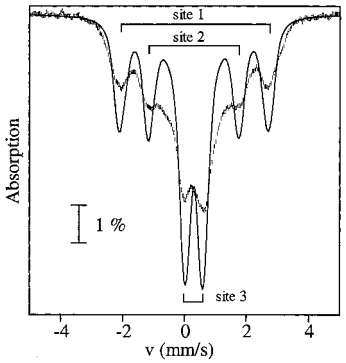

Figure 9. Mössbauer spectrum of *Dg* FdII recorded at 4.2 K in a field of 60 mT applied parallel to the observed γ-radiation. The solid line is a theoretical spectrum obtained for $J_{13} = 300$ cm^{-1}, $J_{12} = 304$ cm^{-1}, $J_{23} = 310$ cm^{-1} and $a_1 = a_2 = a_3 = -18.5$ MHz. For the quoted *J*-values the three sites have very different, but isotropic, *A*-values; see Figure 1. In parallel applied field the nuclear $\Delta m = 0$ lines are quenched and each site produces a four-line spectrum with a 3:1:1:3 intensity pattern. The outermost lines of each subsite are marked by the brackets. (As long as we are only concerned with the $S = {}^1/_2$ ground doublet, the same theoretical spectra are obtained when all three *J*-values are multiplied with the constant factor.)

A-values). A large variation of J_{23}, in turn, leads to a large variation of δ, eq 5, and thus to a large spread of $g_\perp$. In contrast, variation of ω by about 0.2 produces substantial changes of the *A*-values but only minor changes in $g_\perp$, suggesting that a fit to the Mössbauer spectra by variation of J_{12} alone will produce a distribution of $g_\perp$-values that is likely too narrow. Since it is impractical to consider distributions of all four parameters, we have chosen to vary only J_{12}, that is, ω, and explored whether a distribution of this parameter can reasonably explain the features of the observed Mössbauer spectra.

Note from the graph of Figure 1 that a site with positive *A*-values (site 2) has sharp features when ω is close to 1, while the spectrum of a site with negative *A*-values (site 1) is sharp when ω is close to zero. If none of the subsite spectra exhibits sharp features, J_{12} is roughly halfway between J_{13} and J_{23}, that is, $\omega \approx 0.5$. Using the preceding argument together with some initial spectral simulations revealed readily that $\omega > 0.7$ for aconitase (see arrow in Figure 1). For *Dg* FdII the component with the largest negative *A*-value has the sharpest features. Moreover, one of the sites, site 3, has a very small *A*-value. These two observations place the average J_{12} value near the point where A_3 changes sign.

To generate the theoretical spectra of Figure 10 B−D, we have produced a large number of subspectra from eq 15 for fixed $J_{13} = 300$ cm^{-1}, $J_{23} = 310$ cm^{-1}, varying J_{12} in steps of 0.5 cm^{-1} over the range $J_{13} < J_{12} < J_{23}$, and keeping $a_1 = a_2 = a_3$. From studies at temperatures above 77 K it is known that $\Delta E_Q = 0.53$ mm/s and from an 8.0 T spectrum recorded at 150 K (not shown) we could infer that the asymmetry parameter $\eta > 0.8$ for all three sites. We have kept all EFG- tensors in the same frame, with the *z*-axis along the direction of **d**. Initially we attempted a Gaussian distribution of J_{12}, but this did not produce good fits to the data. We have therefore used again the least-squares fitting procedure to determine the distribution of J_{12} values that best fit the entire data set. The final spectra, consisting of a set of three times eight subspectra with the weights listed in the figure caption, are shown in Figure 10 B−D.

Overall, the shapes of the spectra are quite well represented by our simple model. It is gratifying to see that the spectra of all sites can be simulated using one isotropic magnetic hyperfine

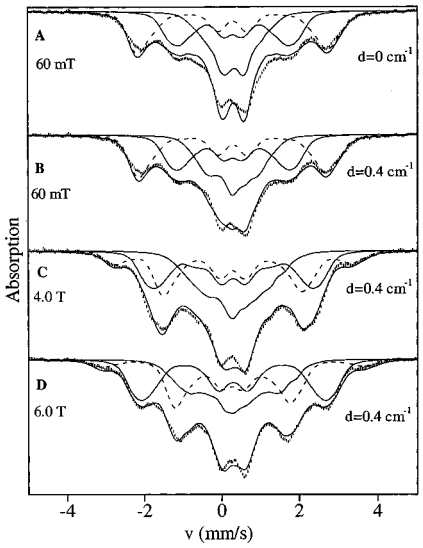

Figure 10. Mössbauer spectra of *Dg* FdII recorded at 4.2 K in parallel applied fields of 0.06 T (A, B), 4.0 T (C), and 6.0 T (D). The solid lines drawn through the data in (B), (C), and (D) are spectral simulations for $d = 0.4$ cm^{-1}, $a_1 = a_2 = a_3 = -18.5$ MHz, $J_{13} = 300$ MHz, $J_{23} = 310$ MHz. J_{12}-values were chosen from 301 to 308 cm^{-1} in steps of 1 cm^{-1}. The theoretical spectra were calculated for the following distribution of J_{12}, combining adjacent points: $J_{12} = 301.5$ (19%), 303.5 (39%), 305.5 (25%), and 307.5 cm^{-1} (17%). We used $\Delta E_Q = 0.52$ mm/s and $\eta = 1$ for all sites. The solid line in (A) is a calculated spectrum for $d = 0$, with all other parameters the same as above.

constant, $a = -18.5$ MHz. All spectra were computed using $d = 0.4$ cm^{-1} for the antisymmetric exchange parameter.

To illustrate the effect of the antisymmetric exchange parameter d we have drawn in Figure 10A a 60 mT spectrum computed for $d = 0$. As anticipated from the argument presented above, the effect of *d* is to broaden preferentially the Mössbauer spectra of sites with smaller effective *A*-values. Since *d* broadens the spectra it is difficult to distinguish its effects from those caused by distributed *J*-values. Thus, we do not claim that the Mössbauer spectra of FdII provide evidence of antisymmetric exchange. However, the effects of this interaction are expressed in the EPR spectra, and if one accepts the interpretation of the EPR spectra, the effect of d on the Mössbauer spectra is roughly as illustrated by the simulations of Figure 10 A and B.

For $d = 0.4$ cm^{-1}, $J_{13} = 300$ cm^{-1}, and $J_{23} = 310$ cm^{-1} one obtains from eq 14 $g_\perp$ values between 1.97 and 1.98 as J_{12} varies between 301 and 308 cm^{-1}, that is, a distribution substantially narrower than indicated by EPR. However, as indicated above we have not employed variations in J_{13}, J_{23}, and *d*. Varying *d* up to 0.6 cm^{-1} would allow $g_\perp$ values down to 1.91 and an additional decrease of $J_{23} - J_{13}$ by only 2 cm^{-1} would allow for $g_\perp$ values down to 1.85, without substantial changes in the Mössbauer spectra.

Discussion

The analyses of the EPR and Mössbauer spectra of aconitase and *Dg* FdII shows that the peculiar spectral features observed for oxidized [3Fe−4S] clusters can be explained by the presence of antisymmetric exchange in combination with heterogeneous distributions of the Heisenberg exchange coupling constants J_{12}, J_{13}, and J_{23}. Our studies show that the occurrence of *g*-values below $g = 2.0$ can be attributed to antisymmetric exchange. This interaction, hitherto not demonstrated for iron−sulfur

clusters, mixes the two lowest $S = {}^1/_2$ manifolds of the spin-coupled cluster and produces **g**-tensors of *axial* symmetry.[35]

Electron spin−lattice relaxation studies[7,20] of a variety of [3Fe−4S] proteins have shown that the two $S = {}^1/_2$ doublets are separated in energy by $\Delta \approx 10-30$ cm^{-1}, depending on the particular system. According to eqs 5 and 13 this splitting reflects, for small *d*-values, the difference in the three *J*-values. Interestingly, the three coupling constants are the same within 1% for aconitase and 3% for *Dg* FdII,[7] in marked contrast, for example, to the all-ferrous [4Fe−4S] cluster of the nitrogenase Fe-protein for which *J*-value differences as large as a factor 2.5 have been inferred.[36]

We are now in the position to address the question why the EPR spectra of *Dg* FdII have broad features that extend down to $g = 1.88$ while those of aconitase are sharp and confined to the region between $g = 2.03$ and 2.00. Both proteins exhibit distributed *J*-values (*J*-strain). For the *Dg* FdII cluster the antisymmetric exchange term of eq 2 moves $g_\perp$ below $g = 2$ and *J*-strain, through the δ-dependence of eq 5, spreads $g_\perp$ over the observed range of *g*-values, but keeping $g_{||}$ at g_0. (We suspect that *d* is distributed as well.) The *d*-value of the aconitase cluster is at least 4 times smaller than that of the FdII cluster, confining its *g*-values to values above $g = 2$ and rendering its EPR spectrum quite insensitive to *J*-strain. However, the broad features of the Mössbauer spectra of aconitase indicate that *J*-strain is present. Duderstadt et al.[8] distinguish between type 1 and type 2 [3Fe−4S]$^+$ clusters; the former have narrow EPR spectra such as aconitase while the latter have broad features such as *Dg* FdII. Our studies suggest that the distinguishing feature between type 1 and 2 is the magnitude of the quantity d/δ.[37] The plots of Figure 8 show that for *Dg* FdII the distribution of $g_\perp$ values peaks near 2.0. For some 3Fe clusters the distribution peaks at lower *g*-values. For instance, using the same method as described above we have analyzed the EPR spectrum of the D14N variant of *Pyroccoccus furious* ferredoxin (shown in Figure 4 of ref 5) and found that its $g_\perp$ distribution peaks around $g_\perp \approx 1.90$, corresponding to $|d|/\delta = 0.025$.

Type 1 [3Fe−4S]$^+$ clusters seem to lack noticeable antisymmetric exchange, and therefore their EPR spectra are confined to *g*-values above $g = 2$. Their spectra are characterized by rhombic *g*-values that appear to reflect the intrinsic rhombicities of the ferric sites. The spectra of the 3Fe clusters of aconitase and the *D. gigas* hydrogenase, $\mathbf{g} = (2.032, 2.024, 2.016)$,[7] represent this type of cluster. It is interesting to note that those type 2 EPR spectra that have been analyzed can be fitted either with distributed rhombic *g*-values or, as shown here, with distributed axial *g*-values. Given the broad nature of the spectra these findings are not too surprising. One might argue that one will generally succeed in fitting the type 2 spectra with distributions of axial species as long as the distributions are not constrained. True rhombic EPR spectra for which the g-value separations are larger than the width of the features at g_x, g_y and g_z produce double-humped distributions when the spectra are represented by axial subspectra. While distributions of rhombic species can fit the data, we are not aware of any mechanism other than mixing by antisymmetric exchange that can shift the *g*-values to values below $g = 2$.

Ideally, we would wish to present fits that use the same distribution of parameters for the computation of the Mössbauer and EPR spectra. As mentioned above, the distributions seem to be batch-dependent thus our ^{57}Fe sample from 1985 is likely to have a distribution of *J*-values different from the EPR sample produced 10 years later.[38] Moreover, as pointed out above the EPR spectrum depends on the distribution of (d^2/δ^2) while the broad features Mössbauer spectra are determined by the distributions of three *J*-values, the antisymmetric exchange parameter *d*, some intrinsic anisotropy of the **A**-tensors, and on (unknown) orientations of the EFG-tensors. While the Mössbauer spectra may be quite sensitive to the distributions of some parameters, it is questionable whether one can work out unique distribution functions from frozen solution samples.

One of the issues that concerned us since the discovery of 3Fe clusters 20 years ago was the apparent anisotropy of the ^{57}Fe magnetic hyperfine tensors. This question has been resolved by the present study which shows that the Mössbauer spectra of aconitase and *Dg* FdII can be fitted with the assumption that the three sites of the cluster have the same isotropic coupling constant, namely $a = -18$ MHz for aconitase and $a = -18.5$ MHz for *Dg* FdII. Mouesca and co-workers[39] have defined a parameter $a_{\text{test}} = \sum_{i=1,3} A_{\text{iso}}(\text{Fe}_i)$ where $A_{iso}(\text{Fe}_i)$ is the measured isotropic part of the magnetic hyperfine tensor. The published magnetic hyperfine tensors of aconitase yielded $a_{\text{test}} = -13$ MHz, a value substantially smaller than expected for a ferric site with tetrahedral sulfur coordination, as noted by Telser et al.[7] The present study resolves this concern and provides a good value for a_{test}, namely $a_{\text{test}} = -(18.0-18.5)$ MHz, for the ferric sites of oxidized [3Fe−4S]$^+$ clusters of the two proteins. The reader should not assume that this study establishes that the **A**-tensors are strictly isotropic. Since the Mössbauer spectra have previously been fitted, and quite well, with anisotropic **A**-tensors it is clear that one can trade some **A**-tensor anisotropy for *J*-strain. We cannot rule out some anisotropy, that is, the **a**-tensor components of aconitase may deviate by ±5% from −18 MHz and those of *Dg* FdII perhaps by ±10% from −18.5 MHz. In fact, Hoffman and co-workers have shown with ENDOR that site 1 of the *Dg* hydrogenase 3Fe cluster has an anisotropic **A**-tensor, $\mathbf{A}_1 = (-51.4, -41.2, -41.2)$ MHz, $A_{\text{iso}} = -44.6$ MHz. This A_{iso}-value indicates that $a_1 \approx -20$ MHz.

The main broadening of the Mössbauer spectra of [3Fe−4S]$^+$ clusters can be attributed to distributed *J*-values that mask the effects of antisymmetric exchange on the spectra. To separate the effects of antisymmetric exchange in the Mössbauer spectra from those associated with distributions of the *J*-values, 3Fe clusters with larger *d*-values or narrower *J*-distributions have to be studied. For instance, to observe effects in the Mössbauer spectra unambiguously attributable to antisymmetric exchange for $d = 0.5$ cm^{-1}, $J_{13} = 300$ cm^{-1}, $J_{23} = 310$ cm^{-1}, and a J_{12} centered at 304 cm^{-1}, the width of the distribution of J_{12} must be less than 0.5 cm^{-1}, that is, less than 0.2% of the absolute value of J_{12}.

For $d = 0$ and well-defined *J*-values the low-temperature Mössbauer spectra provide the quantity $\omega = (J_{12} - J_{13})/(J_{23} - J_{13})$ but not the absolute *J*-values. The value of ω can then be inserted into eq 5 to extract $J_{23} - J_{13}$ from the quantity Δ ($\approx \delta$), measured for instance by spin−lattice relaxation studies. This

(35) This is true as long as mixing of the $S = {}^1/_2$ ground state with $S = {}^3/_2$ manifolds can be neglected. For $J_{ij} > 200$ cm^{-1} and $|d| < 1$ cm^{-1} this condition is fulfilled.

(36) Yoo, S. J.; Angove, H. C.; Burgess, B. K.; Hendrich, M. P.; Münck, E. *J. Am. Chem. Soc.* **1999**, *121*, 2534−2545.

(37) It has been suggested[8] that the broader features of the type 2 clusters suggest less symmetric *J*-coupling. As discussed above less symmetric *J*-coupling alone will not produce broadening of the EPR spectra. For broadening to occur noticeable antisymmetric exchange must be present. Moreover, as can be seen from eqs 5 and 14, larger differences in the J_{ij} will yield larger δ-values and therefore less broadening.

(38) We have just started to investigate systematically for *Dg* FdII the dependence of the distributions on buffer, pH, presence of cryo-protectants and freezing rates.

(39) Mouesca J.-M.; Noodleman, L.; Case, D. A.; Lamotte. B. *Inorg. Chem.* **1995**, *34*, 4347−4359.

still leaves the overall magnitude of the *J*-values undetermined. The *J*-values can be determined from magnetic susceptibility studies, provided they are small enough so that the $S = {}^3/_2$ multiplets are sufficiently populated at the temperatures of the measurement. However, as indicated by the study of Day et al.[21] *J*-values around 300 cm^{-1} are difficult to measure for protein-bound 3Fe-clusters; these authors could only establish a lower bound for the *J*-values of *Dg* FdII, namely $J_{ij} > 200$ cm^{-1}. Analysis of the contact shifts of the cysteinyl protons by NMR[17,18,22] holds great promise for the determination of *J*, provided that the isotropic proton hyperfine coupling constants are known from studies such as electron spin−echo envelope modulation (ESEEM) or ENDOR.[40] Determination of the proton coupling constants by the latter techniques, however, depends on the knowledge of spin projection factors, that is, on the parameter ω. Clearly, determination of the *J*-values of 3Fe clusters requires information from a variety of related techniques, such as EPR, Mössbauer, ENDOR, ESEEM, and NMR spectroscopies and magnetic susceptibility. It is interesting to note that the room-temperature NMR spectra of *Dg* FdII do not exhibit the heterogeneities observed in the low-temperature EPR and Mössbauer spectra; this can be inferred from a comparison of the observed line widths[12,17] with the widths predicted from the *J*-value distribution obtained at low temperature. This observation suggests that the observed *J*-strain, which presumably represents a distribution of protein conformations "locked in" upon freezing the samples, is averaged out in the liquid state. (It is interesting to note that the [4Fe-4S]$^+$ ferredoxin from *Pyrococcus furiosus* exhibits physical mixtures of S = 1/2 and S = 3/2 statues in frozen solution whereas only an S = 1/2 form is observed in fluid solution.[41])

The value found for the AS coupling constant, $d \approx 0.4$ cm^{-1}, is somewhat smaller than the *d*-values reported for the hydroxylase component of methane monooxygenase, $d \approx 2.2$ cm^{-1},[27] a diferric model complex for diiron proteins, $d \approx 1.4$ cm^{-1},[27] and iron triacetate, $d \approx 1.4$ cm^{-1}.[26] Moskvin and Bostrem[42] have reported a microscopic theory of antisymmetric exchange for explaining the experimental data of $Fe^{3+}-Fe^{3+}$ ion pairs in orthoferrites. These authors have shown that the Dzyaloshinskii vector **d** can be written as $\mathbf{d} = d(\vartheta)[\mathbf{r}_{10} \times \mathbf{r}_{20}]$ where $\mathbf{r}_{10}$ and $\mathbf{r}_{20}$ are the unit vectors of the $Fe^{3+}(1)$-O and $Fe^{3+}(2)$-O bonds and ϑ is the Fe^{3+}-O-Fe^{3+} angle. Thus **d** is always perpendicular to the Fe^{3+}-O-Fe^{3+} bond or vanishes for collinear superexchange pathways. The quantity $d(\vartheta)$ depends on transfer integrals, and d was found to differ from the simple relation $d \approx (\Delta g/g)J$ proposed by Moriya.[43] It will be interesting to develop this theory further for the geometrically more complex case of [3Fe−4S]$^+$ clusters.

Acknowledgment. We thank Dr. Michael P. Hendrich for making available to us his EPR simulation routines. We also like to thank Dr. Karl E. Kauffmann for suggestions during the earlier phases of this work. We thank Professor M. Eremin for alerting us to the theoretical work of Moskvin and Bostrem. This work was supported by National Institutes of Health Grant GM-22701.

JA002658I

(40) Doan, P. E.; Fan, C.; Hoffman, B. M. *J. Am. Chem. Soc.* **1994**, *116*, 1033−1041.

(41) Telser, J.; Davydov, R.; Kim, C.-H.; Adams, M. W. W.; Hoffman, B. M. *Inorg. Chem.* **1999**, *38*, 3550−3553.

(42) Moskvin, A. S.; Bostrem, I. G. *Sov. Phys. Solid State* **1977**, *19*, 1532−1538.

(43) Moriya, T. *Phys. Rev.* **1960**, *120*, 91−98.